

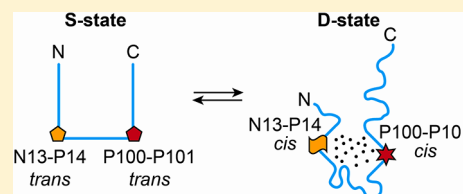
# Metamorphic Protein IscU Changes Conformation by *cis*–*trans* Isomerizations of Two Peptidyl–Prolyl Peptide Bonds

Ziqi Dai,<sup>†</sup> Marco Tonelli,<sup>‡</sup> and John L. Markley<sup>\*,‡</sup>

<sup>†</sup>Graduate Program in Biophysics and <sup>‡</sup>National Magnetic Resonance Facility at Madison and Department of Biochemistry, University of Wisconsin—Madison, Madison, Wisconsin 53706, United States

## S Supporting Information

**ABSTRACT:** IscU from *Escherichia coli*, the scaffold protein for iron–sulfur cluster biosynthesis and transfer, populates two conformational states with similar free energies and with lifetimes on the order of 1 s that interconvert in an apparent two-state reaction. One state (S) is structured, and the other (D) is largely disordered; however, both play essential functional roles. We report here nuclear magnetic resonance studies demonstrating that all four prolyl residues of apo-IscU (P14, P35, P100, and P101) are *trans* in the S state but that two absolutely conserved residues (P14 and P101) become *cis* in the D state. The peptidyl–prolyl peptide bond configurations were determined by analyzing assigned chemical shifts and were confirmed by measurements of nuclear Overhauser effects. We conclude that the  $S \rightleftharpoons D$  interconversion involves concerted *trans*–*cis* isomerization of the N13–P14 and P100–P101 peptide bonds. Although the D state is largely disordered, we show that it contains an ordered domain that accounts for the stabilization of two high-energy *cis* peptide bonds. Thus, IscU may be classified as a metamorphic protein.



Iron–sulfur (Fe–S) cluster proteins are central to many cellular activities, including nitrogen fixation, metabolic catalysis, regulation of gene expression, and electron transfer.<sup>1–3</sup> The machinery that generates Fe–S clusters is highly conserved across all species. Bacteria can contain three Fe–S cluster assembly systems: Nif (nitrogen fixation), Isc (iron–sulfur cluster), and Suf (sulfur formation). Of these, the Isc system is responsible for assembling and delivering clusters for most iron–sulfur proteins in bacteria and also is operational in the mitochondria of eukaryotes.<sup>1</sup> Defects in the Isc machinery underlie aging processes and a number of human diseases.<sup>4–7</sup> IscU (Isu1 and Isu2 in yeast and ISCU in human) is the scaffold protein on which the iron–sulfur cluster is assembled and delivered to receiver apoproteins. IscU interacts with most of the other proteins in the Isc pathway, including the cysteine desulfurase that donates sulfur<sup>8–11</sup> and the specialized DnaK/DnaJ-type cochaperone pair that facilitates cluster transfer in vivo in an ATP-dependent mechanism.<sup>12–14</sup>

IscU from *Escherichia coli* populates two interconverting conformational states. One state (S) is structured and has yielded an NMR structure (PDB entry 2L4X),<sup>15</sup> and the other (D) is dynamically disordered and lacks the secondary structural elements found in the S state.<sup>16,17</sup> At pH 8.0 and 25 °C, the  $S \rightarrow D$  rate is 0.77 s<sup>–1</sup> and the  $D \rightarrow S$  rate is 2.0 s<sup>–1</sup>.<sup>17</sup> Both states have been shown to be functionally essential in that the D state is the substrate for the cysteine desulfurase IscS<sup>17</sup> and is the form present in the HscA–IscU complex,<sup>18</sup> whereas the S state binds preferentially to the DnaJ-type cochaperone HscB<sup>16,18</sup> and also is the conformational state of the protein when it contains a [2Fe–2S] cluster.<sup>19</sup> Because residues observed by NMR spectroscopy exhibit two separate peaks corresponding to the S and D states,<sup>16,17</sup> the interconversion appears to be a two-state process.

We suspected that a peptidyl–prolyl *cis*–*trans* isomerization might account for the slow step in the interconversion. We report

here NMR studies showing that all four prolyl residues of apo-IscU (P14, P35, P100, and P101) are *trans* in the S state but that two (P14 and P101) become *cis* in the D state. The two prolyl residues involved are strictly conserved in the sequences of all IscU proteins (see Figure S1 of the Supporting Information). Proline at position 101 has been shown to be essential for recognition by the Hsp70-type chaperone HscA,<sup>20</sup> and substitution of the homologous proline for alanine in yeast Isu led to a slow growth phenotype.<sup>21</sup> These results imply that the D state, which supports two high-energy *cis* peptide bonds, cannot be fully disordered. This expectation is confirmed by heteronuclear NOE results that show that the D state contains ordered and disordered domains. We conclude that IscU has evolved to interconvert between two conformational states that serve different functions in the cycle of iron–sulfur cluster assembly and delivery.

## EXPERIMENTAL PROCEDURES

**Protein Production and Purification.** Labeled amino acids were purchased from Cambridge Isotope Laboratories (Andover, MA). [U-<sup>13</sup>C,<sup>15</sup>N-Pro]IscU and [U-<sup>13</sup>C,<sup>15</sup>N-Pro,U-<sup>15</sup>N-Ala]-IscU were prepared according to a modification of a published procedure.<sup>22</sup> A colony of BL21 cells transformed with the pTrc 99A plasmid containing the IscU gene was used to inoculate 5 mL of TB liquid medium containing 100 µg/mL ampicillin. The cells were grown overnight at 37 °C, and a 100 µL aliquot was used to inoculate 250 mL of TB liquid medium containing 100 µg/mL ampicillin. This culture was grown for 12 h at 37 °C. Cells isolated from this 250 mL culture by centrifugation were used to

Received: October 17, 2012

Revised: October 29, 2012

Published: October 30, 2012



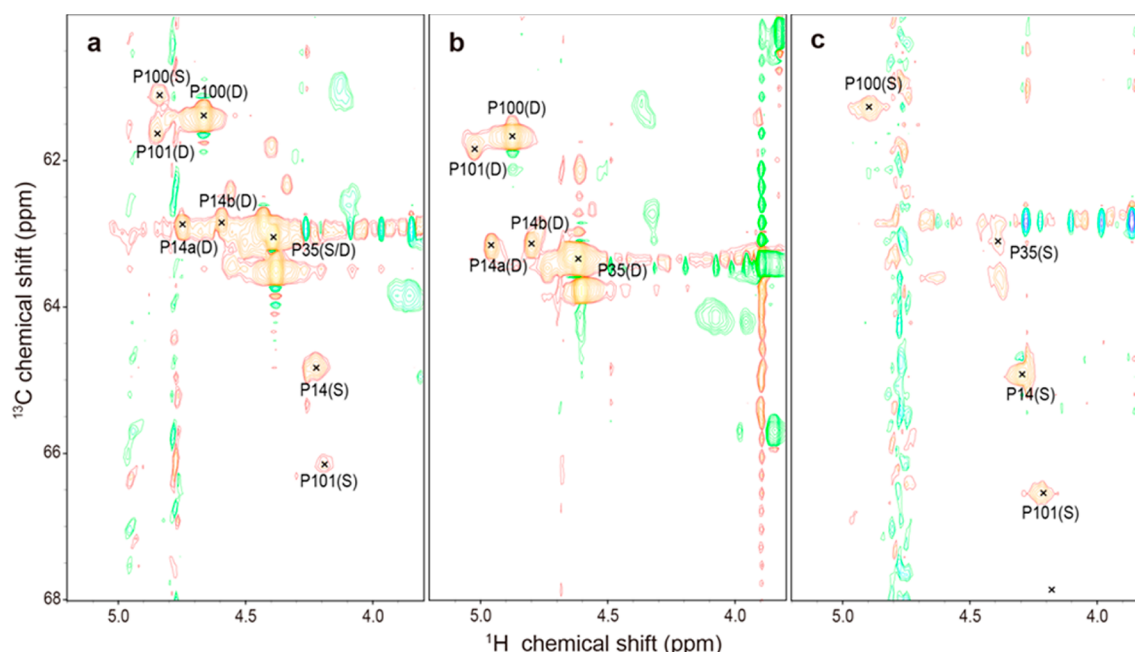


**Figure 1.** Aliphatic regions of 2D  $^1\text{H}$ – $^{13}\text{C}$  HSQC spectra of 1 mM  $[\text{U-}^{13}\text{C}, ^{15}\text{N-Pro}]$ IscU acquired at 600 MHz ( $^1\text{H}$ ) under the conditions specified. (a) Spectrum of apo-IscU acquired at pH 8.0 and 25 °C, where the protein is a mixture of the S and D states. (b) Spectrum of apo-IscU acquired at 45 °C, where the protein is in the D state. (c) Spectrum of the Zn-bound form of IscU acquired at pH 8.0 and 25 °C, where the protein is in the S state. Assignments to individual prolyl residues were determined as described in the text. Each NMR sample for panels a and b contained 1 mM  $[\text{U-}^{13}\text{C}, ^{15}\text{N-Pro}]$ IscU, 50 mM Tris-HCl (pH 8.0), 0.5 mM EDTA, 5 mM DTT, 150 mM NaCl, 50  $\mu\text{M}$  DSS, and 50  $\mu\text{M}$   $\text{NaN}_3$  in 10%  $\text{D}_2\text{O}$ . The NMR sample for panel c contained 1 mM  $[\text{U-}^{13}\text{C}, ^{15}\text{N-Pro}]$ IscU: $\text{Zn}^{2+}$ , 50 mM Tris-HCl (pH 8.0), 5 mM DTT, 150 mM NaCl, 50  $\mu\text{M}$  DSS, and 50  $\mu\text{M}$   $\text{NaN}_3$  in 10%  $\text{D}_2\text{O}$ .

inoculate 1000 mL of M9 medium containing 100  $\mu\text{g}/\text{mL}$  ampicillin and supplemented with 1 mL of a vitamin solution,<sup>22</sup> 1 g of  $\text{NH}_4\text{Cl}$ , and 4 g of glucose and a cocktail containing the labeled amino acids to be incorporated along with unlabeled amino acids.<sup>23</sup>  $[\text{U-}^{15}\text{N}]$ IscU and  $[\text{U-}^{13}\text{C}, \text{U-}^{15}\text{N}]$ IscU were prepared in a similar fashion, except that the medium contained, as needed, 1 g of  $[\text{U-}^{15}\text{N}]\text{NH}_4\text{Cl}$ , 3 g of  $[\text{U-}^{13}\text{C}]\text{glucose}$ , and no labeled amino acids. The culture was induced when the  $\text{OD}_{600}$  reached  $\approx 1$  via addition of IPTG to a final concentration of 0.4 mM. Protein was purified as described previously.<sup>22,24</sup> The elution buffer consisted of 50 mM Tris-HCl (pH 8.0), 1 mM DTT, 0.5 mM EDTA, and 150 mM NaCl. Fractions were analyzed by gel electrophoresis, and those appearing to be homogeneous were pooled, concentrated by ultrafiltration, frozen in liquid nitrogen, and stored at  $-80^\circ\text{C}$ . The isotopic labeling efficiency as determined by mass spectrometry was  $\sim 92\%$ .  $\text{Zn}^{2+}$ -bound IscU was prepared by gradually adding aliquots from a stock buffer containing 50 mM Tris-HCl (pH 8.0), 10 mM  $\text{ZnCl}_2$ , and 150 mM NaCl to a solution of apo-IscU.

**NMR Spectroscopy and Data Analysis.** DSS was used as an internal reference for all NMR chemical shift measurements. NMR data were collected at the National Magnetic Resonance Facility at Madison (NMRFAM) on Varian VNMRs spectrometers equipped with z-gradient cryogenic probes. NMRPipe<sup>25</sup> was used to process the raw NMR data. SPARKY<sup>26</sup> was used for data analysis. The resonance assignments of apo-IscU were based in part on previous results.<sup>16,17</sup>

**Data Deposition.** Assigned chemical shifts acquired at 45 and 25 °C in the presence of  $\text{Zn}^{2+}$  have been deposited in the BioMagResBank as entries 18754 and 18750, respectively.

## RESULTS

**Proline NMR Peak Assignments.** The two-dimensional (2D)  $^1\text{H}$ – $^{13}\text{C}$  HSQC NMR spectrum of  $[\text{U-}^{13}\text{C}, ^{15}\text{N-Pro}]$ IscU

**Table 1. Signals Observed in the 3D HACAN Spectrum of  $([\text{U-}^{13}\text{C}, ^{15}\text{N}]\text{Pro}, [\text{U-}^{13}\text{C}, ^{15}\text{N}]\text{Ala})\text{IscU}:\text{Zn}^{2+}$  That Led to the Assignment of Signals to the Four Prolyl Residues in the S State**

residue <sup>a</sup>	$^{15}\text{N}$ signal visible from $^1\text{H}^\alpha$ – $^{13}\text{C}^\alpha$ peaks	$^1\text{H}^\alpha$ – $^{13}\text{C}^\alpha$ peaks visible from $^{15}\text{N}$ signals
Pro14	$\text{H}^\alpha_{\text{P14}}-\text{C}^\alpha_{\text{P14}}-\text{N}_{\text{P14}}$	$\text{H}^\alpha_{\text{P14}}-\text{C}^\alpha_{\text{P14}}-\text{N}_{\text{P14}}$
Pro35	$\text{H}^\alpha_{\text{P35}}-\text{C}^\alpha_{\text{P35}}-\text{N}_{\text{P35}}$	$\text{H}^\alpha_{\text{P35}}-\text{C}^\alpha_{\text{P35}}-\text{N}_{\text{P35}}$
Ala36	$\text{H}^\alpha_{\text{P35}}-\text{C}^\alpha_{\text{P35}}-\text{N}_{\text{A36}}$	$\text{H}^\alpha_{\text{P35}}-\text{C}^\alpha_{\text{P35}}-\text{N}_{\text{A36}}$
Pro100	$\text{H}^\alpha_{\text{P100}}-\text{C}^\alpha_{\text{P100}}-\text{N}_{\text{P100}}$	$\text{H}^\alpha_{\text{P100}}-\text{C}^\alpha_{\text{P100}}-\text{N}_{\text{P101}}$
Pro101	$\text{H}^\alpha_{\text{P100}}-\text{C}^\alpha_{\text{P100}}-\text{N}_{\text{P101}}$	$\text{H}^\alpha_{\text{P100}}-\text{C}^\alpha_{\text{P100}}-\text{N}_{\text{P101}}$
	$\text{H}^\alpha_{\text{P101}}-\text{C}^\alpha_{\text{P101}}-\text{N}_{\text{P101}}$	$\text{H}^\alpha_{\text{P101}}-\text{C}^\alpha_{\text{P101}}-\text{N}_{\text{P101}}$

<sup>a</sup>The strict conservation of these residues is illustrated in Figure S1 of the Supporting Information.

(IscU produced biosynthetically with incorporation of proline labeled with the stable isotopes  $^{13}\text{C}$  and  $^{15}\text{N}$ ) recorded at pH 8.0 and 25 °C, where both the S and D states are populated at an  $[\text{S}]/[\text{D}]$  ratio of  $\sim 2.6$ , revealed a single set of peaks for P35, two sets of peaks for P100 and P101, and three sets of peaks for P14 (Figure 1a). To observe peaks from the S state alone, we added  $\text{Zn}^{2+}$ , which constrains the protein to the S state,<sup>17</sup> and collected data at 25 °C (Figure 1c). To observe peaks from the D state alone, we took advantage of the temperature dependence of the  $\text{S} \rightleftharpoons \text{D}$  equilibrium, which shifts toward the D state at higher temperatures so that at 45 °C only signals from the D state were observed (Figure 1b). Plots of the same data at lower contour levels did not reveal any additional signals from prolyl residues (Figure S2 of the Supporting Information).

To assign signals to the four individual prolyl residues, we prepared a selectively labeled sample of IscU by biosynthetic

Table 2. NMR Assignments for the Prolyl Residues of the S and D States of IscU

IscU state	residue	chemical shift (ppm)				$\delta^{13}\text{C}^\beta - \delta^{13}\text{C}^\gamma$ (ppm)	peptide bond configuration
		$^{13}\text{C}^\alpha$	$^1\text{H}^\alpha$	$^{13}\text{C}^\beta$	$^{13}\text{C}^\gamma$		
structured (S)	Pro14	64.79	4.226	31.98	27.35	4.63	<i>trans</i>
	Pro35	63.06	4.410	32.05	27.40	4.65	<i>trans</i>
	Pro100	61.16	4.845	30.91	27.08	3.83	<i>trans</i>
	Pro101	66.13	4.204	32.03	27.45	4.58	<i>trans</i>
disordered (D)	Pro14a	62.95	4.743	34.45	24.82	9.63	<i>cis</i>
	Pro14b	62.91	4.597	34.34	24.73	9.61	<i>cis</i>
	Pro35	63.06	4.410	32.05	27.40	4.65	<i>trans</i>
	Pro100	61.36	4.667	30.88	27.36	3.52	<i>trans</i>
	Pro101	61.50	4.848	33.07	24.74	8.33	<i>cis</i>

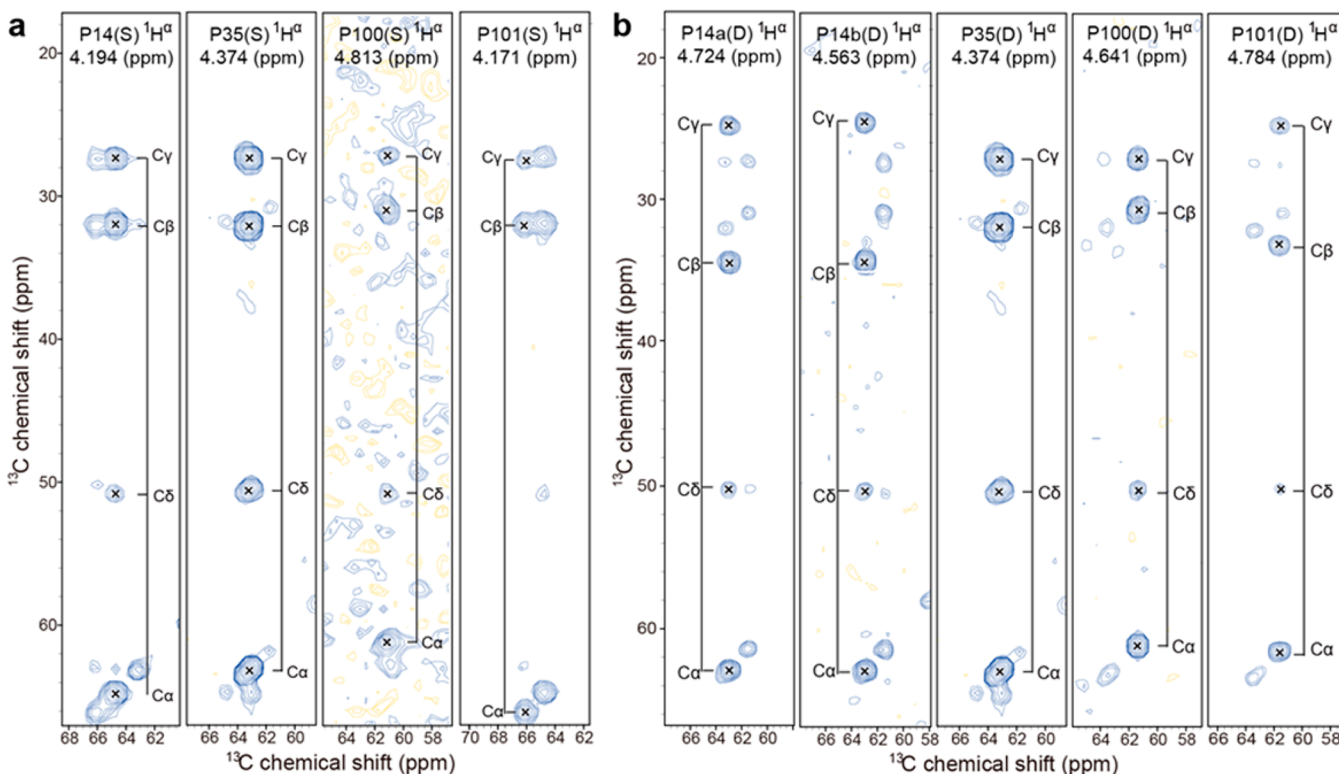


**Figure 2.** 2D strip plots from 3D (H)CCH-TOCSY spectra of IscU acquired at 600 MHz ( $^1\text{H}$ ). The NMR sample contained 1 mM  $[\text{U-}^{13}\text{C}, ^{15}\text{N-Pro}] \text{IscU}$ , 50 mM Tris-HCl (pH 8.0), 5 mM DTT, 150 mM NaCl, 50  $\mu\text{M}$  DSS, and 50  $\mu\text{M}$   $\text{NaN}_3$  in 10%  $\text{D}_2\text{O}$ . 2D strips were taken at the chemical shifts of the prolyl  $^1\text{H}^\alpha$ , shown at the top of each strip. (a) Spectrum of the S state of IscU stabilized as the  $\text{Zn}^{2+}$  complex at 25 °C. (b) Spectra of the D state of IscU acquired at 45 °C.

incorporation of  $[\text{U-}^{13}\text{C}, ^{15}\text{N}] \text{Pro}$  and  $[\text{U-}^{15}\text{N}] \text{Ala}$ . This labeling pattern allowed us to identify the spin system of P35 from the P35  $^{13}\text{C}^\alpha\text{--A36 } ^{15}\text{N}$  connectivity, the spin systems of P100 and P101 from the P100  $^{13}\text{C}^\alpha\text{--P101 } ^{15}\text{N}$  connectivity, and the spin system of P14 by exclusion. To identify these connectivities in the S state, we collected a three-dimensional (3D) HACAN spectrum<sup>27</sup> of the  $\text{Zn}^{2+}$  complex, which allowed the observation of signals from the  $^1\text{H}^\alpha\text{--}^{13}\text{C}^\alpha$  signal of residue  $i$  to its own nitrogen ( $^1\text{H}^\alpha\text{--}^{13}\text{C}^\alpha\text{--}^{15}\text{N}_i$ ) and to the nitrogen of the adjacent residue  $i + 1$  ( $^1\text{H}^\alpha\text{--}^{13}\text{C}^\alpha\text{--}^{15}\text{N}_{i+1}$ ) (Table 1). Because the prolyl residues were the only ones labeled uniformly with  $^{13}\text{C}$  and  $^{15}\text{N}$  and because P100 and P101 constitute the sole P-P sequence in IscU, P101 is the only residue whose nitrogen yielded two sets of prolyl  $^1\text{H}^\alpha\text{--}^{13}\text{C}^\alpha$  signals. We were thus able to unambiguously identify signals from P101 from the  $^1\text{H}^\alpha_{\text{P100}}\text{--}^{13}\text{C}^\alpha_{\text{P100}}\text{--}^{15}\text{N}_{\text{P101}}$  connectivity (Table 1). Moreover, because the sample contained  $[\text{U-}^{15}\text{N}] \text{Ala}$ , we assigned signals to P35 from the observed  $^1\text{H}^\alpha_{\text{P35}}\text{--}^{13}\text{C}^\alpha_{\text{P35}}\text{--}^{15}\text{N}_{\text{A36}}$  connectivity in the 3D HACAN

**Table 3. Predictions of *cis* Xaa–Pro Bond Likelihood for *E. coli* IscU by the Promega Server<sup>31</sup> from Amino Acid Sequence and Chemical Shift Data**

state	residue	likelihood for Pro to be <i>cis</i>	normalized likelihood for Pro to be <i>cis</i>
structured (S)	Pro14	0.000	0.000
	Pro35	0.000	0.000
	Pro100	0.000	0.000
	Pro101	0.000	0.000
disordered (D)	Pro14a	1.000	0.998
	Pro14b	1.000	0.998
	Pro35	0.001	0.000
	Pro100	0.001	0.000
	Pro101	0.999	0.988

spectrum (Table 1). The remaining  $^1\text{H}^\alpha\text{--}^{13}\text{C}^\alpha\text{--}^{15}\text{N}$  peak in the spectrum was assigned to P14 ( $^1\text{H}^\alpha_{\text{P14}}\text{--}^{13}\text{C}^\alpha_{\text{P14}}\text{--}^{15}\text{N}_{\text{P14}}$ ).

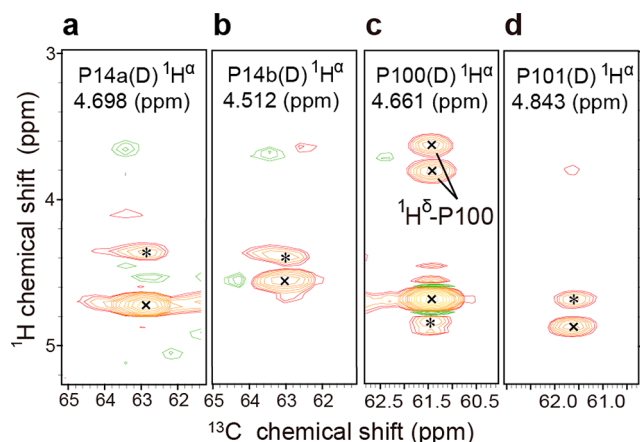


**Figure 3.** 3D  $^{13}\text{C}$ -edited 900 MHz ( $^1\text{H}$ ) NOESY data acquired at 45 °C at a mixing time of 125 ms, which confirm that the P100–P101 and N13–P14 peptide bonds of IscU are in the *cis* form in the D state. The sample contained 1 mM [ $^{13}\text{C}$ ,  $^{15}\text{N}$ -Pro]IscU, 50 mM Tris-HCl (pH 8.0), 0.5 mM EDTA, 5 mM DTT, 150 mM NaCl, 50  $\mu\text{M}$  DSS, and 50  $\mu\text{M}$   $\text{NaN}_3$  in 10%  $\text{D}_2\text{O}$ . Peaks labeled with an x are diagonal peaks; peaks labeled with an asterisk are NOE peaks. (a) 2D strip at the  $^1\text{H}^\alpha$  chemical shift of P14a; the NOE peak is from (N13) $^1\text{H}^\alpha \cdots ^1\text{H}^\alpha - ^{13}\text{C}^\alpha$ (P14a). (b) 2D strip at the  $^1\text{H}^\alpha$  chemical shift of P14b; the NOE peak is from (N13) $^1\text{H}^\alpha \cdots ^1\text{H}^\alpha - ^{13}\text{C}^\alpha$ (P14b). (c) 2D strip at the  $^1\text{H}^\alpha$  chemical shift of P100; the NOE peak is from (P101) $^1\text{H}^\alpha \cdots ^1\text{H}^\alpha - ^{13}\text{C}^\alpha$ (P100). The peaks at  $^1\text{H}$  chemical shifts of 3.6 and 3.8 ppm arise from NOEs from (P100) $^1\text{H}^\alpha$  to  $^1\text{H}^{\delta 2}$  and  $^1\text{H}^{\delta 3}$  of P100 and/or P101. (d) 2D strip at the  $^1\text{H}^\alpha$  chemical shift of P101; the NOE peak is from (P100) $^1\text{H}^\alpha \cdots ^1\text{H}^\alpha - ^{13}\text{C}^\alpha$ (P101).

The same strategy was used to assign the proline signals of the D state, except that the IscU sample contained no  $\text{Zn}^{2+}$  and data were collected at 45 °C. Although a single set of peaks was observed for P14 in the S state ( $^1\text{H}^\alpha$  at 4.226 ppm and  $^{13}\text{C}^\alpha$  at 64.79 ppm), two sets of peaks corresponding to P14 in the D state were found: one with  $^1\text{H}^\alpha$  at 4.743 ppm and  $^{13}\text{C}^\alpha$  at 62.94 ppm and the other with  $^1\text{H}^\alpha$  at 4.597 ppm and  $^{13}\text{C}^\alpha$  at 62.91 ppm. We refer to these two sets of peaks as P14a and P14b, respectively (see Figure 1b). The origin of this local structural heterogeneity remains to be determined.

**Prolyl Peptide Bond Configurations from NMR Chemical Shifts.** Previous studies of peptidyl–prolyl *cis*–*trans* isomerization have shown that prolyl residues with *cis* peptide bonds typically have  $^{13}\text{C}^\beta$  signals around 25 ppm and  $^{13}\text{C}^\gamma$  signals near 35 ppm, where  $\delta^{13}\text{C}^\gamma - \delta^{13}\text{C}^\beta \approx 10$  ppm; conversely, prolyl residues with *trans* peptide bonds typically have  $^{13}\text{C}^\beta$  signals around 27 ppm and  $^{13}\text{C}^\gamma$  signals near 32 ppm, where  $\delta^{13}\text{C}^\gamma - \delta^{13}\text{C}^\beta \approx 5$  ppm.<sup>28–32</sup> We determined the chemical shifts of the  $^{13}\text{C}$  atoms of each prolyl residue from 3D (H)CCH TOCSY spectra (Table 2). When the protein was in the S state, the chemical shift difference ( $\delta^{13}\text{C}^\gamma - \delta^{13}\text{C}^\beta$ ) for all four prolyl residues was  $\sim 5$  ppm, indicating that they are all *trans* (Figure 2a). However, when the protein was in the D state, the chemical shift difference was  $\sim 5$  ppm for P35 and P100, showing that they remain *trans*, but  $\sim 10$  ppm for P14a, P14b, and P101, indicating that they have become *cis* (Figure 2b).

An algorithm has been developed (implemented in the Promega program) for calculation of the statistical probability of a *trans* or *cis*

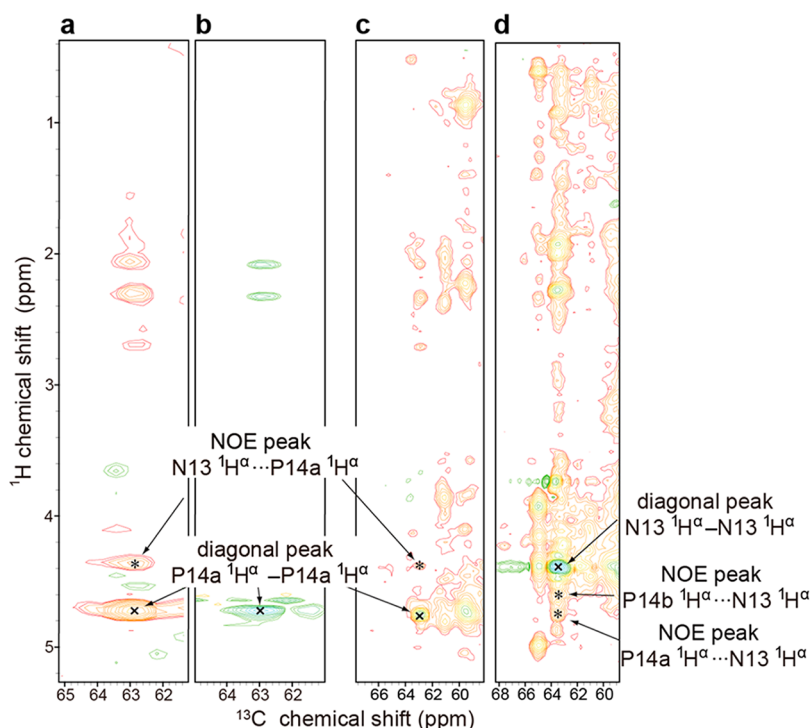


**Figure 4.** NMR spectra collected at 900 MHz ( $^1\text{H}$ ) and 45 °C where the protein is in the D state. The NMR samples contained 1 mM protein, 50 mM Tris-HCl (pH 8.0), 0.5 mM EDTA, 5 mM DTT, 150 mM NaCl, 50  $\mu\text{M}$  DSS, and 50  $\mu\text{M}$   $\text{NaN}_3$  in 10%  $\text{D}_2\text{O}$ . Diagonal peaks are marked with an x and NOE peaks with an asterisk. (a) Strip at the P14a  $^1\text{H}^\alpha$  chemical shift from a 3D  $^{13}\text{C}$ -edited  $^1\text{H}$ – $^1\text{H}$  NOESY spectrum (mixing time of 125 ms) of [ $^{13}\text{C}$ ,  $^{15}\text{N}$ -Pro]IscU. (b) Strip at the P14a  $^1\text{H}^\alpha$  chemical shift from a 3D H(C)CH-TOCSY spectrum of [ $^{13}\text{C}$ ,  $^{15}\text{N}$ -Pro]IscU. The cross-peak matches the  $^1\text{H}^\alpha - ^{13}\text{C}^\alpha$  position of the diagonal in panel A. (c) Strip at the P14a  $^1\text{H}^\alpha$  chemical shift from a 3D  $^{13}\text{C}$ -edited  $^1\text{H}$ – $^1\text{H}$  NOESY spectrum (mixing time of 125 ms) of [ $^{13}\text{C}$ ,  $^{15}\text{N}$ ]IscU. The uniformly labeled sample exhibits cross-peaks at the same positions as those from the selectively labeled sample (panel a). (d) Strip at the N13  $^1\text{H}^\alpha$  chemical shift from a 3D  $^{13}\text{C}$ -edited  $^1\text{H}$ – $^1\text{H}$  NOESY spectrum (mixing time of 125 ms) of [ $^{13}\text{C}$ ,  $^{15}\text{N}$ ]IscU. Both P14a  $^1\text{H}^\alpha$  and P14b  $^1\text{H}^\alpha$  exhibit NOEs with N13  $^1\text{H}^\alpha$ .



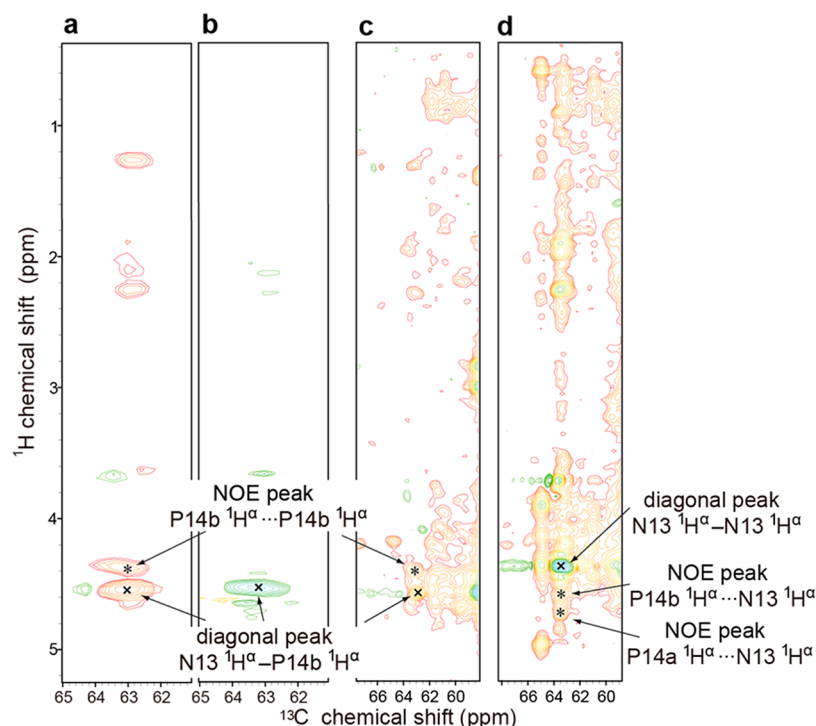


**Figure 5.** NMR spectra collected at 900 MHz ( $^1\text{H}$ ) and 45  $^\circ\text{C}$  where the protein is in the D state. The NMR samples contained 1 mM protein, 50 mM Tris-HCl (pH 8.0), 0.5 mM EDTA, 5 mM DTT, 150 mM NaCl, 50  $\mu\text{M}$  DSS, and 50  $\mu\text{M}$   $\text{NaN}_3$  in 10%  $\text{D}_2\text{O}$ . Diagonal peaks are marked with an x and NOE peaks with an asterisk. (a) Strip at the P14b  $^1\text{H}^\alpha$  chemical shift from a 3D  $^{13}\text{C}$ -edited  $^1\text{H}$ – $^1\text{H}$  NOESY spectrum (mixing time of 125 ms) of  $[\text{U-}^{13}\text{C}, ^{15}\text{N-Pro}] \text{IscU}$ . (b) Strip at the P14b  $^1\text{H}^\alpha$  chemical shift from a 3D H(C)CH-TOCSY spectrum of  $[\text{U-}^{13}\text{C}, ^{15}\text{N-Pro}] \text{IscU}$ . The cross-peak matches the  $^1\text{H}^\alpha$ – $^{13}\text{C}^\alpha$  position of the diagonal in panel a. (c) Strip at the P14b  $^1\text{H}^\alpha$  chemical shift from a 3D  $^{13}\text{C}$ -edited  $^1\text{H}$ – $^1\text{H}$  NOESY spectrum (mixing time of 125 ms) of  $[\text{U-}^{13}\text{C}, ^{15}\text{N}] \text{IscU}$ . The uniformly labeled sample exhibits cross-peaks at the same positions as those from the selectively labeled sample (panel a). (d) Same spectrum as panel d in Figure S2 of the Supporting Information. Strip at the N13  $^1\text{H}^\alpha$  chemical shift from a 3D  $^{13}\text{C}$ -edited  $^1\text{H}$ – $^1\text{H}$  NOESY spectrum of  $[\text{U-}^{13}\text{C}, ^{15}\text{N}] \text{IscU}$ . Both P14a  $^1\text{H}^\alpha$  and P14b  $^1\text{H}^\alpha$  exhibit NOEs with N13  $^1\text{H}^\alpha$ .

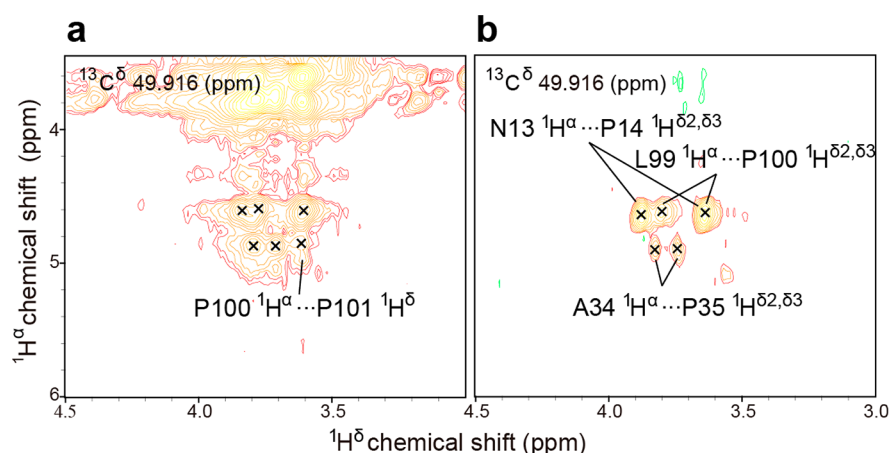


**Figure 6.** 900 MHz ( $^1\text{H}$ ) spectra of  $[\text{U-}^{13}\text{C}, ^{15}\text{N-Pro}] \text{IscU}$  at 25  $^\circ\text{C}$  in the presence of  $\text{Zn}^{2+}$  where the protein is in the S state. The NMR sample contained 1 mM protein, 1 mM  $\text{ZnCl}_2$ , 50 mM Tris-HCl (pH 8.0), 5 mM DTT, 150 mM NaCl, 50  $\mu\text{M}$  DSS, and 50  $\mu\text{M}$   $\text{NaN}_3$  in 10%  $\text{D}_2\text{O}$ . (a) 2D strip from a 3D  $^{13}\text{C}$ -edited  $^1\text{H}$ – $^1\text{H}$  NOESY spectrum without filtration (mixing time of 125 ms). (b) 3D  $^{13}\text{C}$ -filtered,  $^{13}\text{C}$ -edited  $^1\text{H}$ – $^1\text{H}$  NOESY spectrum (mixing time of 125 ms) showing only NOE cross-peaks between protons attached to  $^{13}\text{C}$  and protons attached to  $^{12}\text{C}$  ( $^{12}\text{C}^\alpha$ – $^1\text{H}^\alpha$ ... $^1\text{H}^\delta$ – $^{13}\text{C}^\delta$  NOEs survive;  $^{13}\text{C}^\alpha$ – $^1\text{H}^\alpha$ ... $^1\text{H}^\delta$ – $^{13}\text{C}^\delta$  NOEs, such as those within the same or between the two prolyl residues, are filtered out).  $^1\text{H}^\alpha$ ... $^1\text{H}^{\delta 2, \delta 3}$  NOE signals from N13–P14, A34–P35, and L99–P100 residue pairs (b) confirm that these peptide bonds are *trans*. The same peaks are observed in the unfiltered spectrum (a). Panel a contains an additional resolved  $^1\text{H}^\alpha$ ... $^1\text{H}^\delta$  NOE peak assigned to the P100–P101 residue pair, which confirms that the peptide bond is *trans*.

Xaa–Pro peptide bond from the sequence of the protein and the prolyl chemical shifts and backbone chemical shifts of neighboring residues.<sup>31</sup> Analysis of our data by this program confirmed the configurations for the prolyl peptide bonds reported above at normalized likelihood values of  $\geq 0.998$  (Table 3).

**Prolyl Peptide Bond Configurations from Nuclear Overhauser Effect (NOE) Measurements.** Another standard way to determine the Xaa–Pro peptide bond configuration is to measure the relative distances between hydrogen atoms on adjacent residues by means of the nuclear Overhauser effect

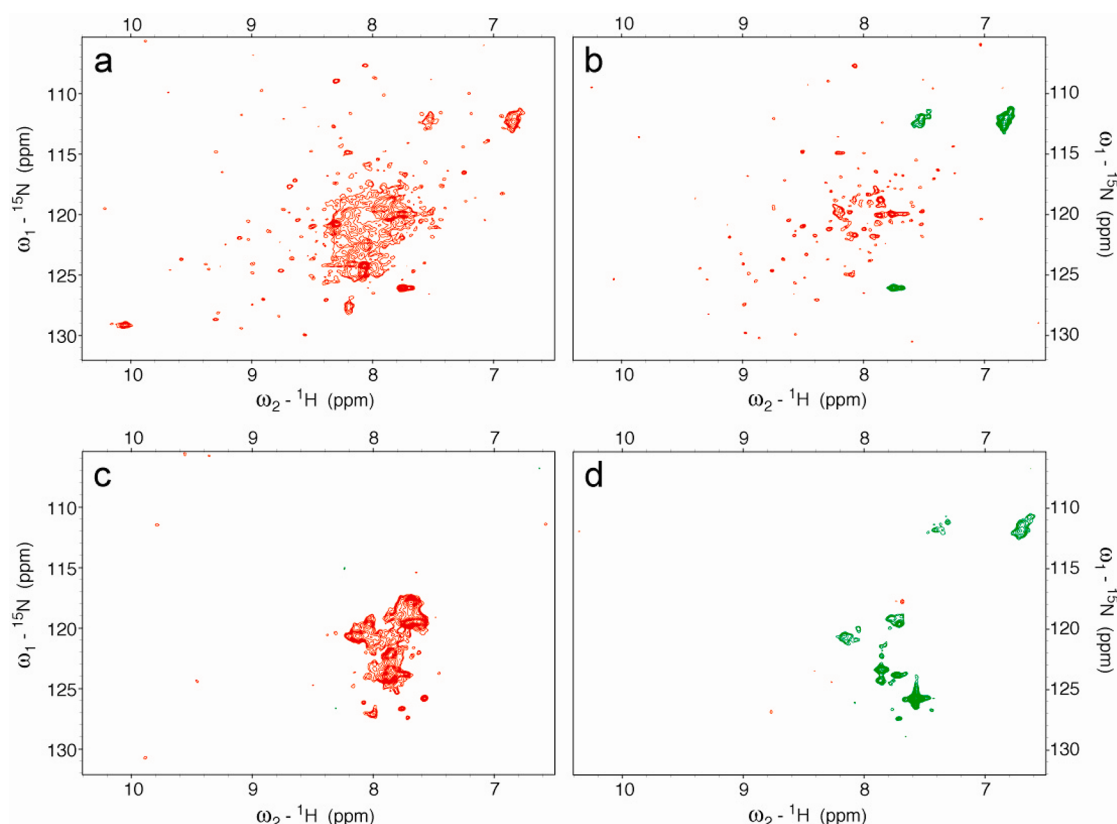


**Figure 7.** 800 MHz  $^1\text{H}$ – $^{15}\text{N}$  HSQC spectra of  $[\text{U}-^{15}\text{N}]\text{IscU}$  at pH 8.0 and different temperatures, with positive peaks colored orange and negative peaks colored green: (a) 45 °C without heteronuclear NOE, (b) 45 °C with heteronuclear NOE, (c) 70 °C without heteronuclear NOE, and (d) 70 °C with heteronuclear NOE.

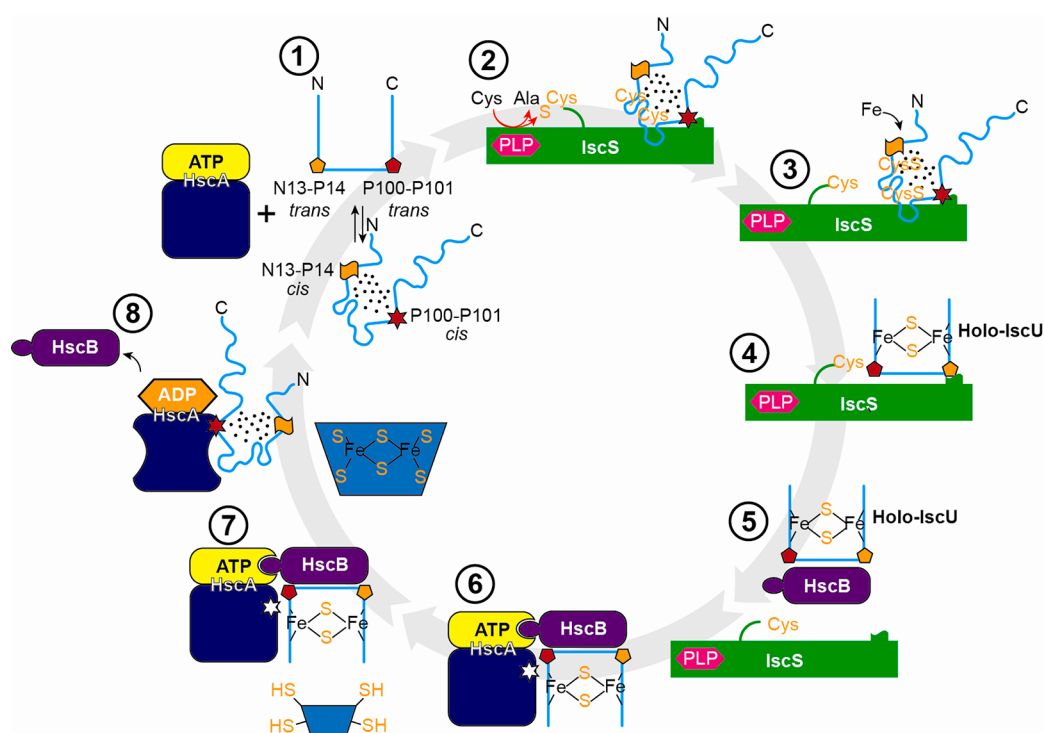


**Figure 8.** Working model for the mechanism of iron–sulfur cluster assembly and transfer. (1) Free IscU in DS equilibrium. (2) Complex of the cysteine desulfurase (IscS) and the D state of IscU. (3) Addition of sulfur to Cys residues of IscU. (4) Addition of iron to form a  $[2\text{Fe}-2\text{S}]$  cluster stabilized by the S state of IscU. (5) Transfer of holo-IscU to the cochaperone (HscB). (6) Docking of holo-IscU to the HscA–ATP complex. (7) Approach of an acceptor apoprotein. (8) Transfer of the Fe–S cluster to the acceptor protein, release of HscB, and binding of the D state of IscU to HscA–ADP. (1) Return to the starting state by exchange of HscA-bound ADP with ATP and release of IscU.

(NOE). In a *trans* peptide bond, the  $H^\alpha$  atom of the preceding residue is close to the prolyl  $H^{\delta 2}$  and  $H^{\delta 3}$  atoms, whereas in a *cis* peptide bond, the  $H^\alpha$  atom of the preceding residue is close to the prolyl  $H^\alpha$  atom (see Figure S3 of the Supporting Information). The 3D  $^{13}\text{C}$ -edited  $^1\text{H}$ – $^1\text{H}$  NOESY spectrum of [ $U\text{-}^{13}\text{C},^{15}\text{N}$ -Pro]-IscU, at 45 °C where the protein is in the D state, exhibited two NOE signals between P100 and P101 indicative of a *cis* peptide bond (Figure 3a):  $H^\alpha_{P101}\cdots H^\alpha_{P100}-C^\alpha_{P100}$  and  $H^\alpha_{P100}\cdots H^\alpha_{P101}-C^\alpha_{P101}$ . The same spectrum exhibited an  $H^\alpha_{N13}\cdots H^\alpha_{P14a}-C^\alpha_{P14a}$  NOE signal between N13 and P14a indicative of a *cis* peptide bond (Figure 3b). Similarly, the  $H^\alpha_{N13}\cdots H^\alpha_{P14b}-C^\alpha_{P14b}$  NOE signal observed between N13 and P14b confirmed a *cis* peptide bond (Figure 3c). Peak assignments were confirmed by reference to data from the 3D H(C)CH TOCSY spectrum of [ $U\text{-}^{13}\text{C},^{15}\text{N}$ -Pro]IscU and 3D  $^{13}\text{C}$ -edited  $^1\text{H}$ – $^1\text{H}$  NOESY spectrum of [ $U\text{-}^{13}\text{C},^{15}\text{N}$ ]IscU (Figures 4 and 5). Comparison of  $^{13}\text{C}$ -edited  $^1\text{H}$ – $^1\text{H}$  NOESY and  $^{13}\text{C}$ -filtered,  $^{13}\text{C}$ -edited  $^1\text{H}$ – $^1\text{H}$  NOESY spectra of IscU in the  $\text{Zn}^{2+}$ -bound S state confirmed the presence of  $^1H^\alpha_{i-1}\cdots\text{prolyl } ^1H^\delta$  NOEs indicative of *trans* peptide bonds for all four prolyl residues (Figure 6).

**Evidence of Partial Order in the D State.** The 800 MHz  $^1\text{H}$ – $^{15}\text{N}$  HSQC spectrum of [ $U\text{-}^{15}\text{N}$ ]IscU recorded at pH 8.0 and 45 °C, where the protein is predominantly in the D state, exhibited a set of overlapped, nondispersed peaks and a set of dispersed peaks (Figure 7a). The signals from nondispersed amide side chains exhibited negative heteronuclear NOEs, whereas the other nondispersed and dispersed signals exhibited positive heteronuclear NOEs (Figure 7b). We attribute the nondispersed peaks to residues in disordered regions of the protein and the dispersed peaks to residues in the fold that stabilizes the two *cis* prolyl peptide bonds. Corresponding spectra recorded at 70 °C (Figure 7c,d) showed only nondispersed peaks with negative heteronuclear NOE values as expected for a fully unfolded protein.

## DISCUSSION

Studies of model peptides have shown that the *trans* configuration of a peptidyl–prolyl peptide bond is favored over the *cis* form by approximately 0.5–1.3 kcal/mol.<sup>33</sup> Thus, the energy required to stabilize two *cis* peptide bonds by at least 95% (to explain the observation of NMR signals from only the *cis* state when IscU is in the D state) is  $\geq 4.5$  kcal/mol, and the stabilization energy may be a major factor in increasing the free energy of the D state so that it is close to that of the S state. NMR spectra collected at 45 °C, where the protein is predominantly in the D state (Figure 7a,b), show that the protein contains regions of both disorder and order. The protein becomes fully unfolded only at higher temperatures (Figure 7c,d). These results show that the D state of IscU is not fully disordered but rather contains an ordered domain that stabilizes two high-energy *cis* peptide bonds.

Thus, IscU can be categorized as a metamorphic protein, one that populates two different conformations with similar free energies that are capable of interconversion under physiological conditions.<sup>34</sup> Prior examples of metamorphic proteins, Mad2<sup>35</sup> and lymphotactin,<sup>36,37</sup> are monomeric in one state and dimeric in the other. By contrast, IscU is monomeric in both states. IscU appears to have evolved to be metamorphic, with the two states playing alternate roles in the cycle of iron–sulfur cluster formation and delivery.

Figure 8 illustrates our working model for the steps in Fe–S cluster formation and delivery, along with schematic representations of states of the peptidyl–prolyl peptide bonds of IscU that undergo changes in configuration. The D state, which is the initial

substrate for the cysteine desulfurase,<sup>17</sup> does not bind metals, leaving the cysteine residues free to accept sulfur to form persulfides. After the delivery of iron, the atoms rearrange to form a  $[2\text{Fe-2S}]$  cluster ligated by four side chains of IscU in its S state (three Cys residues and one His residue).<sup>19</sup> Product inhibition is minimized because the S state of IscU binds less strongly to the cysteine desulfurase than the D state. HscB binds more tightly to the S state than the D state,<sup>16,18</sup> which ensures its selective binding to holo-IscU. HscB targets the HscB–holo-IscU complex to the ATP-bound form of the chaperone protein HscA. Following ATP hydrolysis, HscA in its R state preferentially binds and stabilizes the D state of IscU,<sup>18</sup> leading to irreversible cluster release. Finally, when the ADP bound to HscA is replaced with ATP, HscA reverts to its T state, and apo-IscU is released.<sup>18</sup> The conformational changes of the scaffold protein IscU accompanied by peptidyl–prolyl bond *cis*–*trans* isomerizations thus serve to increase the efficiency of iron–sulfur cluster formation and delivery. Because the free energies of the S and D states are similar, very little of the binding energy is required to shift the equilibrium.

## ASSOCIATED CONTENT

### Supporting Information

Alignment of sequences of IscU proteins illustrating their conservation (Figure S1), NMR spectra from Figure 1 plotted at a lower contour level (Figure S2), and representations of *trans* and *cis* peptidyl–prolyl peptide bonds illustrating the expected NOEs (Figure S3). This material is available free of charge via the Internet at <http://pubs.acs.org>.

## AUTHOR INFORMATION

### Corresponding Author

\*Telephone: (608) 263-9349. E-mail: [markley@nmrfam.wisc.edu](mailto:markley@nmrfam.wisc.edu).

### Funding

This work was supported by National Institutes of Health (NIH) Grants R01 GM58667 and U01 GM94622 in collaboration with the National Magnetic Resonance Facility at Madison, which is supported by NIH grants from the National Center for Research Resources (5P41RR002301-27 and RR02301-26S1) and the National Institute for General Medical Sciences (8P41 GM103399-27).

### Notes

The authors declare no competing financial interest.

## ABBREVIATIONS

DSS, 4,4-dimethyl-4-silapentane-1-sulfonic acid; EDTA, 2,2',2'',2'''-(ethane-1,2-diyl)dinitrilo)tetraacetic acid; HSQC, heteronuclear single-quantum correlation; NMR, nuclear magnetic resonance; NOE, nuclear Overhauser enhancement; PDB, Protein Data Bank.

## REFERENCES

- (1) Ayala-Castro, C.; Saini, A.; Outten, F. W. (2008) Fe–S cluster assembly pathways in bacteria. *Microbiol. Mol. Biol. Rev.* 72, 110–125.
- (2) Johnson, M. K. (1998) Iron-sulfur proteins: New roles for old clusters. *Curr. Opin. Chem. Biol.* 2, 173–181.
- (3) Rees, D. C., and Howard, J. B. (2003) The interface between the biological and inorganic worlds: Iron-sulfur metallocusters. *Science* 300, 929–931.
- (4) Campuzano, V.; Montermini, L.; Molto, M. D.; Pianese, L.; Cossee, M.; Cavalcanti, F.; Monros, E.; Rodius, F.; Duclos, F.; Monticelli, A.; Zara, F.; Canizares, J.; Koutnikova, H.; Bidichandani, S. I.; Gellera, C.; Brice, A.; Trouillas, P.; De Michele, G.; Filla, A.; De Frutos, R.; Palau, F.; Patel, P. I.; Di Donato, S.; Mandel, J. L.; Coccozza, S.; Koenig, M.; and Pandolfo, M. (1996) Friedreich's ataxia: Autosomal recessive disease

caused by an intronic GAA triplet repeat expansion. *Science* 271, 1423–1427.

(5) Rouault, T. A., and Tong, W. H. (2008) Iron-sulfur cluster biogenesis and human disease. *Trends Genet.* 24, 398–407.

(6) Sheftel, A., Stehling, O., and Lill, R. (2010) Iron-sulfur proteins in health and disease. *Trends Endocrinol. Metab.* 21, 302–314.

(7) Shi, Y., Ghosh, M. C., Tong, W. H., and Rouault, T. A. (2009) Human ISD11 is essential for both iron-sulfur cluster assembly and maintenance of normal cellular iron homeostasis. *Hum. Mol. Genet.* 18, 3014–3025.

(8) Kato, S., Mihara, H., Kurihara, T., Takahashi, Y., Tokumoto, U., Yoshimura, T., and Esaki, N. (2002) Cys-328 of IscS and Cys-63 of IscU are the sites of disulfide bridge formation in a covalently bound IscS/IscU complex: Implications for the mechanism of iron-sulfur cluster assembly. *Proc. Natl. Acad. Sci. U.S.A.* 99, 5948–5952.

(9) Nuth, M., and Cowan, J. A. (2009) Iron-sulfur cluster biosynthesis: Characterization of IscU-IscS complex formation and a structural model for sulfide delivery to the [2Fe-2S] assembly site. *J. Biol. Inorg. Chem.* 14, 829–839.

(10) Shi, R., Proteau, A., Villarroja, M., Moukadiri, I., Zhang, L., Trempe, J. F., Matte, A., Armengod, M. E., and Cygler, M. (2010) Structural basis for Fe-S cluster assembly and tRNA thiolation mediated by IscS protein-protein interactions. *PLoS Biol.* 8, e1000354.

(11) Zhang, W., Urban, A., Mihara, H., Leimkuhler, S., Kurihara, T., and Esaki, N. (2010) IscS functions as a primary sulfur-donating enzyme by interacting specifically with MoeB and MoaD in the biosynthesis of molybdopterin in *Escherichia coli*. *J. Biol. Chem.* 285, 2302–2308.

(12) Cupp-Vickery, J. R., and Vickery, L. E. (2000) Crystal structure of Hsc20, a J-type Co-chaperone from *Escherichia coli*. *J. Mol. Biol.* 304, 835–845.

(13) Hoff, K. G., Ta, D. T., Tapley, T. L., Silberg, J. J., and Vickery, L. E. (2002) Hsc66 substrate specificity is directed toward a discrete region of the iron-sulfur cluster template protein IscU. *J. Biol. Chem.* 277, 27353–27359.

(14) Vickery, L. E., and Cupp-Vickery, J. R. (2007) Molecular chaperones HscA/Ssq1 and HscB/Jac1 and their roles in iron-sulfur protein maturation. *Crit. Rev. Biochem. Mol. Biol.* 42, 95–111.

(15) Kim, J. H., Tonelli, M., Kim, T., and Markley, J. L. (2012) Three-Dimensional Structure and Determinants of Stability of the Iron-Sulfur Cluster Scaffold Protein IscU from *Escherichia coli*. *Biochemistry* 51, 5557–5563.

(16) Kim, J. H., Füžéry, A. K., Tonelli, M., Ta, D. T., Westler, W. M., Vickery, L. E., and Markley, J. L. (2009) Structure and dynamics of the iron-sulfur cluster assembly scaffold protein IscU and its interaction with the cochaperone HscB. *Biochemistry* 48, 6062–6071.

(17) Kim, J. H., Tonelli, M., and Markley, J. L. (2012) Disordered form of the scaffold protein IscU is the substrate for iron-sulfur cluster assembly on cysteine desulfurase. *Proc. Natl. Acad. Sci. U.S.A.* 109, 454–459.

(18) Kim, J. H., Tonelli, M., Frederick, R. O., Chow, D. C., and Markley, J. L. (2012) Specialized Hsp70 Chaperone (HscA) Binds Preferentially to the Disordered Form, whereas J-protein (HscB) Binds Preferentially to the Structured Form of the Iron-Sulfur Cluster Scaffold Protein (IscU). *J. Biol. Chem.* 287, 31406–31413.

(19) Shimomura, Y., Kamikubo, H., Nishi, Y., Masako, T., Kataoka, M., Kobayashi, Y., Fukuyama, K., and Takahashi, Y. (2007) Characterization and crystallization of an IscU-type scaffold protein with bound [2Fe-2S] cluster from the hyperthermophile, *Aquifex aeolicus*. *J. Biochem.* 142, 577–586.

(20) Tapley, T. L., Cupp-Vickery, J. R., and Vickery, L. E. (2006) Structural determinants of HscA peptide-binding specificity. *Biochemistry* 45, 8058–8066.

(21) Dutkiewicz, R., Schilke, B., Cheng, S., Kniesner, H., Craig, E. A., and Marszalek, J. (2004) Sequence-specific interaction between mitochondrial Fe-S scaffold protein Isu and Hsp70 Ssq1 is essential for their in vivo function. *J. Biol. Chem.* 279, 29167–29174.

(22) Hoff, K. G., Silberg, J. J., and Vickery, L. E. (2000) Interaction of the iron-sulfur cluster assembly protein IscU with the Hsc66/Hsc20

molecular chaperone system of *Escherichia coli*. *Proc. Natl. Acad. Sci. U.S.A.* 97, 7790–7795.

(23) Cheng, H., Westler, W. M., Xia, B., Oh, B. H., and Markley, J. L. (1995) Protein expression, selective isotopic labeling, and analysis of hyperfine-shifted NMR signals of *Anabaena* 7120 vegetative [2Fe-2S] ferredoxin. *Arch. Biochem. Biophys.* 316, 619–634.

(24) Füžéry, A. K., Tonelli, M., Ta, D. T., Cornilescu, G., Vickery, L. E., and Markley, J. L. (2008) Solution structure of the iron-sulfur cluster cochaperone HscB and its binding surface for the iron-sulfur assembly scaffold protein IscU. *Biochemistry* 47, 9394–9404.

(25) Delaglio, F., Grzesiek, S., Vuister, G. W., Zhu, G., Pfeifer, J., and Bax, A. (1995) NMRPIPE: A Multidimensional Spectral Processing System Based on UNIX Pipes. *J. Biomol. NMR* 6, 277–293.

(26) Goddard, T. D., and Kneller, D. G. (2010) *Sparky 3*, University of California, San Francisco.

(27) Kanelis, V., Donaldson, L., Muhandiram, D. R., Rotin, D., Forman-Kay, J. D., and Kay, L. E. (2000) Sequential assignment of proline-rich regions in proteins: Application to modular binding domain complexes. *J. Biomol. NMR* 16, 253–259.

(28) Dorman, D. E., Torchia, D. A., and Bovey, F. A. (1973) Carbon-13 and proton nuclear magnetic resonance observations of the conformation of poly(L-proline) in aqueous salt solutions. *Macromolecules* 6, 80–82.

(29) Howarth, O. W., and Lilley, D. M. J. (1978) Carbon-13-NMR of Peptides and Proteins. *Prog. Nucl. Magn. Reson. Spectrosc.* 12, 1–40.

(30) Schubert, M., Labudde, D., Oschkinat, H., and Schmieder, P. (2002) A software tool for the prediction of Xaa-Pro peptide bond conformations in proteins based on <sup>13</sup>C chemical shift statistics. *J. Biomol. NMR* 24, 149–154.

(31) Shen, Y., and Bax, A. (2010) Prediction of Xaa-Pro peptide bond conformation from sequence and chemical shifts. *J. Biomol. NMR* 46, 199–204.

(32) Siemion, I. Z., Wieland, T., and Pook, K. H. (1975) Influence of the distance of the proline carbonyl from the β and γ carbon on the <sup>13</sup>C chemical shifts. *Angew. Chem., Int. Ed.* 14, 702–703.

(33) Grathwohl, C., and Wüthrich, K. (1981) NMR Studies of the Rates of Proline cis–trans Isomerization in Oligopeptides. *Biopolymers* 20, 2623–2633.

(34) Murzin, A. G. (2008) Biochemistry: Metamorphic proteins. *Science* 320, 1725–1726.

(35) Mapelli, M., Massimiliano, L., Santaguida, S., and Musacchio, A. (2007) The Mad2 conformational dimer: Structure and implications for the spindle assembly checkpoint. *Cell* 131, 730–743.

(36) Kuloglu, E. S., McCaslin, D. R., Markley, J. L., and Volkman, B. F. (2002) Structural rearrangement of human lymphotactin, a C chemokine, under physiological solution conditions. *J. Biol. Chem.* 277, 17863–17870.

(37) Tyler, R. C., Murray, N. J., Peterson, F. C., and Volkman, B. F. (2011) Native-state interconversion of a metamorphic protein requires global unfolding. *Biochemistry* 50, 7077–7079.